Combustion and Flame 281 (2025) 114304

Contents lists available at ScienceDirect

Combustion and Flame

journal homepage: www.sciencedirect.com/journal/combustion-and-flame

Consumable embedded microwave Antenna in AP/HTPB propellant to focus energy at the reaction front

Keren Shi, Erik Hagen, Yujie Wang, Michael R. Zachariah *

University of California, Riverside, CA, 92521, USA

ARTICLE INFO

Keywords:
Solid propellant
Microwave
Combustion modulation

ABSTRACT

This study demonstrates a novel method to modulate the burn rate of AP/HTPB propellants by embedding a *consumable* microwave (MW) antenna, which can be directly coupled to a MW source. The tip of the antenna, which is being consumed, is thus always at the burning surface of the propellant and radiates MW energy to weakly absorbing HTPB. We found a significant increase in burn rate (up to ~2X), with increasing MW power, despite the fact that the flame temperatures were unaffected. These results indicated that the function of the antenna was restricted to delivering power to the condensed phase. Electric field simulation indicates that the MW energy focused at the burning surface and along the axial direction along the MW antenna. This study shows that focusing on MW energy on the burning surface can be used to modulate burn rate of propellants by embedding a consumable MW antenna.

1. Introduction

Solid propellants are widely used as boosters due to the simple motor design, relatively low cost and stability [1–3]. It is common to boost the energy release rate by adding metal particles such as Aluminum [4,5]. However, once ignited, the premixed fuel and oxidizer are designed to maintain self-sustained combustion, without the ability to throttle. Lasers have been used as a method to stimulate the burning surface of solid propellant [6,7], but often due to poor coupling (e.g. AP/HTPB), other additives such as carbon black are added [8]. Barkley et al. employed microwave (MW) stimulation to the Al/AP/HTPB system with $NaNO_3$ dopants to couple MW energy to the gas phase flame [9]. They proposed major mechanisms including: MW-plasma flame enhancement by inelastic electron-neutral collisions, oxide thermal runaway absorption by the Al droplet and volumetric heating of the condensed phase of propellant. Lajoie et al. have further explored the dielectric heating on the solid propellant by MW in AP/HTPB/ethylene glycol propellants and pretreated propellants prior to ignition to increase the porosity and an increase in burn rate [10].

In our previous study, we incorporated a receiving antenna embedded within a poor MW absorbing Aluminum/Copper Oxide nanocomposite. Using a monopole antenna emitter, localized hotspots could be generated at the two terminals of the embedded receiving antenna, resulting from the high induced electric field intensity [11,12]. By tuning the induced electric field intensity at the receiving antenna, ignition and local modulation of the burn rate could be achieved. Simulation of the electric field of a monopole antenna for that study shows how the electric field is focused at the tip (Fig. 1(a)). This work follows from this simulation and provides the motivation for the concept to embed an MW antenna within a MW sensitive solid propellant, parallel to the direction of intended propagation. In this conceptualization, the tip of the antenna is always at the burning surface and is consumed so as to maintain the maximum field at the surface of the burning propellant.

In this work, we explored this idea by embedding a thin tin wire within an AP/HTPB propellant to act as a MW antenna. HTPB weakly absorbs MW energy, while AP is MW transparent [13,14]. The tin wire is shown to be fine enough that heat conduction was not a contributing factor in the behavior of the propellant. The low melting point of tin ensured that the tip was maintained at the burning surface during propagation. Local burn rate measurements showed a linear increase with MW power, up to ~2X in our experiments. Imaging pyrometry suggested that the flame temperature was not affected by MW stimulation. Simulation of electric field distribution in the propellant indicated that HTPB was heated by the emitted electric field from MW antenna at the burning surface and along the axial direction of MW antenna. Analysis of a quenched sample suggested MW heating did not cause propellant decomposition, and no void formation was observed. This

* Corresponding author.
E-mail address: mrz@engr.ucr.edu (M.R. Zachariah).

https://doi.org/10.1016/j.combustflame.2025.114304
Received 21 January 2025; Received in revised form 12 June 2025; Accepted 14 June 2025
Available online 6 September 2025

experiment provides a novel and safe method to modulate the local burn rate of AP/HTPB propellants by embedding a MW antenna. This method offers a strategy to throttle a solid propellant by focusing MW energy on the burning surface.

2. Experiment

2.1. Materials

Hydroxyl-terminated Polybutadiene Resin (HTPB, OH value: 0.81), Methylene Diphenyl Diisocyanate (MDI, modified curative) and Isodecyl pelargonate plasticizer (IDP) were purchased from Rocket Motor Components Inc. Ammonium Perchlorate (AP, 90 μm) was obtained from Pyro Chemical Source LLC. Tin wire (Chip Quik, diameter: 150 μm) was used as the MW antenna embedded within the propellant.

2.2. Propellants with MW antenna fabrication

The propellants with MW antenna were fabricated by a cast molding method. First, ~1568 mg of HTPB was mixed with ~232 mg MDI and ~200 mg IDP in a planetary mixer (Thinky AR100) at 2000 rpm for 5 mins. Then ~4666 mg of AP was added and mixed at 2000 rpm for 10 mins. The MW antenna was fixed along the axis of a cylindrical Teflon mold (diameter: 45 mm), and the mixture was injected into the mold and cured for 72 h. The weight percentage of AP was ~70 % in the cured propellant. The propellants with MW antenna were prepared in three different lengths (~20 mm, ~40 mm and ~60 mm) for further tests. The propellant cross-section with MW antenna is shown in Figure S1.

2.3. Microwave stimulated propellant combustion

The propellants with MW antenna were soldered to coaxial connectors (Amphenol RF) and connected to the MW source before combustion experiments. The MW source consists of a magnetron (MKS Instruments, TM012/MKS50, frequency 2.45 GHz, λ ~122 mm), a dual channel MW directional coupler (MKS Instruments, DC2340) connected to a MW power sensor (MKS Instruments, RD8400), an MW tuner (MKS Instruments, AG340) and a WR340 cavity to coaxial transition adaptor (MEGA RF Solutions). The experiment scheme is shown in Fig. 1(b). The power delivered to the MW antenna was measured by a vector network analyzer (Keysight N9918A) [11]. The propellants with MW antenna were tested under ambient conditions and were ignited at the top. Then the MW was turned on and set at two levels (76 ± 2 W and 160 ± 7 W) during combustion, and the process was recorded by a color camera (Vision Research Phantom, Miro M110, exposure time 100 μs, spatial resolution ~45–55 μm per pixel).

2.4. Burn rate and flame temperature measurement

To obtain the local burn rate change with time (t), the position of the burning surface (x) was extracted from color camera video frames. The flame temperature during the combustion was measured by three color pyrometry [15,16]. This method uses ratios of the intensities from the red, green and blue channels of the color camera, which was calibrated against a calibrated black body source (Mikron M390). The temperature uncertainty is estimated to be ~200–300 K. The images at first and last 5 mm of propellants were not used for local burn rate and flame temperature analysis to eliminate edge effect.

2.5. Heat transfer simulation

A heat transfer model was developed using the COMSOL Multiphysics 5.6 package to estimate the effect of the embedded MW antenna (Tin wire) on the burn rate without MW stimulation [17]. The model included metal wire (diameter: 150 μm, length: 40 mm) in the center and surrounded by the propellant (diameter: 4.5 mm, length: 40 mm) (Figure S2). The burning surface temperature was set as 800 K [18]. The thermal properties of the Tin and Aluminum (Al) were obtained from COMSOL built-in library, and the thermal properties of the propellant were calculated from 70 wt. % of AP and 30 wt. % of HTPB (MDI and IDP are assumed to have the same thermal properties as HTPB, detailed thermal properties were listed in Table S1) [10].

2.6. Electric field simulation

COMSOL Multiphysics 5.6 was used to simulate the electric field distribution in the solid propellant, using the same geometry at the heat transfer model [17]. The surrounding air was not included, and the out surface of the propellant was set as transparent to scattered waves. The power input port is set at the bottom of the antenna, at 76 W and 160 W as measured by the VNA. The relative permeability of the solid propellant was 1, and the relative permittivity of the solid propellant was 1.26

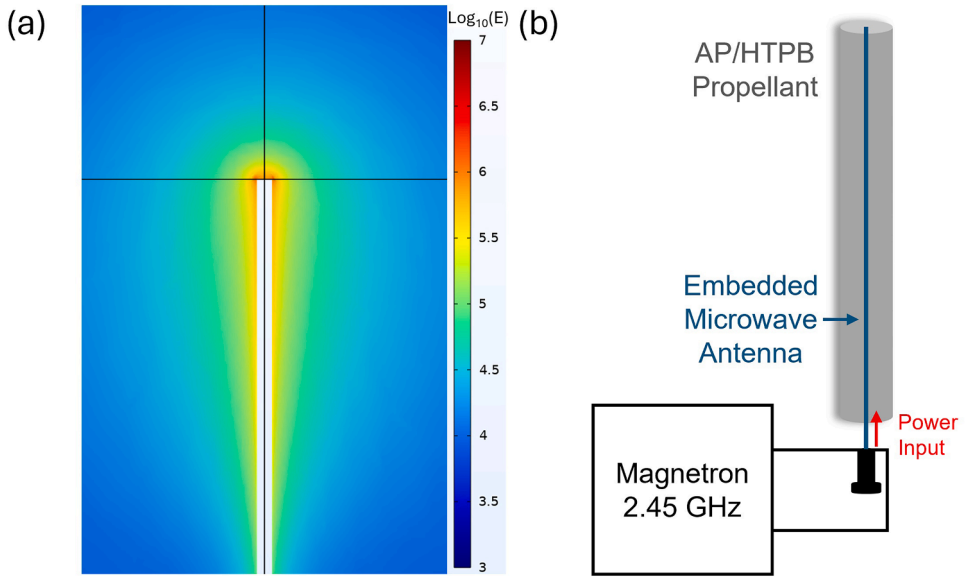

Fig. 1. (a) Near field electric field (unit: V/m) simulation of a monopole antenna [11]. The electric field showed highest intensity at the tip of antenna and decreased along the MW antenna. (b) Scheme of the MW stimulated propellant combustion setup.

– 0.0024j (calculated from volume percent average of 30 wt. % HTPB and 70 wt. % AP, the relative permittivity of MDI and IDP are assumed to be the same as HTPB) [10,19]. The parameters of tin were from COMSOL built-in library.

2.7. Burnt propellant characterization

To assess the MW heating effect on the propellants, the 60 mm samples were quenched when ~5 mm were still remaining in the burn (with and without MW). The samples were cut into slices and the cross-sections were examined under an optical microscope to evaluate the integrity of propellants under MW heating.

3. Results and discussion

3.1. Burn rate modulation by MW stimulation

Embedding a metal wire inside a solid propellant has previously been studied as a method to improve burn rate of solid propellant. In those studies, metal with high thermal conductivity such as copper or aluminum showed an increase in burn rate and was attributed to heat conduction by the wire [20–22]. In order to ensure this would not occur as a confounding effect we employed a much finer wire (150 μm). Our propagation experiments showed that adding the fine wire barely changed the burn rate: 1.30 ± 0.04 mm/s vs. 1.28 ± 0.11 mm/s without the wire. In other words, the wire itself had no influence on the burn rate. To further convince ourselves a heat transfer model was developed to quantify the heat conduction from the embedded wire to the propellant. Using available thermal properties we see in Figure S3 that for a tin wire of 150 μm, and imposing a burning surface temperature of 800 K, that radial heat conduction from the wire is minimal. The results showed that the heat transfer effects may become important when the wire diameter exceeds 250 μm. This also explains why prior work with larger diameters > 500 μm showed acceleration in burn rate due solely to heat transfer effects [20].

The effect of the MW stimulation was tested by first igniting the 40 mm propellants with an embedded MW antenna, and then powering on the MW at different power levels. The images of the propellants with MW antenna at same time intervals show that the burn rate increased with higher MW power (Fig. 2(a) to (d)). The local burn rate of 40 mm propellants with embedded MW antenna are shown in Fig. 2(e).

Two important features stand out,

1. The burn rate is clearly very sensitive to MW power.
2. The local burn rate under MW stimulation increases with the burn time (MW stimulation time), something unexpected and will be explained later.

These trends are also observed for different strand lengths of 20 and 60 mm as presented in Fig. 3. The longest samples showed the most enhancement as evidenced by the 60 mm sample which showed a ~2X increase. During propellant combustion, we saw no evidence of the tin wire extending above the burning surface, implying the original design concept of a consumable wire was born out. Thus, the tip of the MW antenna was always synced with the burning surface position where the electric field is maximum.

3.2. Mechanism of burn rate increase

MW can interact with the solid propellant systems in two potential ways. First is the MW can ionize gas phase species generated, and create plasma [9,23]. Plasma formation and the increases energy input from MW provides a higher flame temperature and thus heat feedback, which often results in higher burn rate. The second mechanism is that the solid components can be directly heated by the MW. The design of this experiment is directed to the second approach.

To further explore the driving force for burn enhancement we observed with microwave we begin with flame temperature

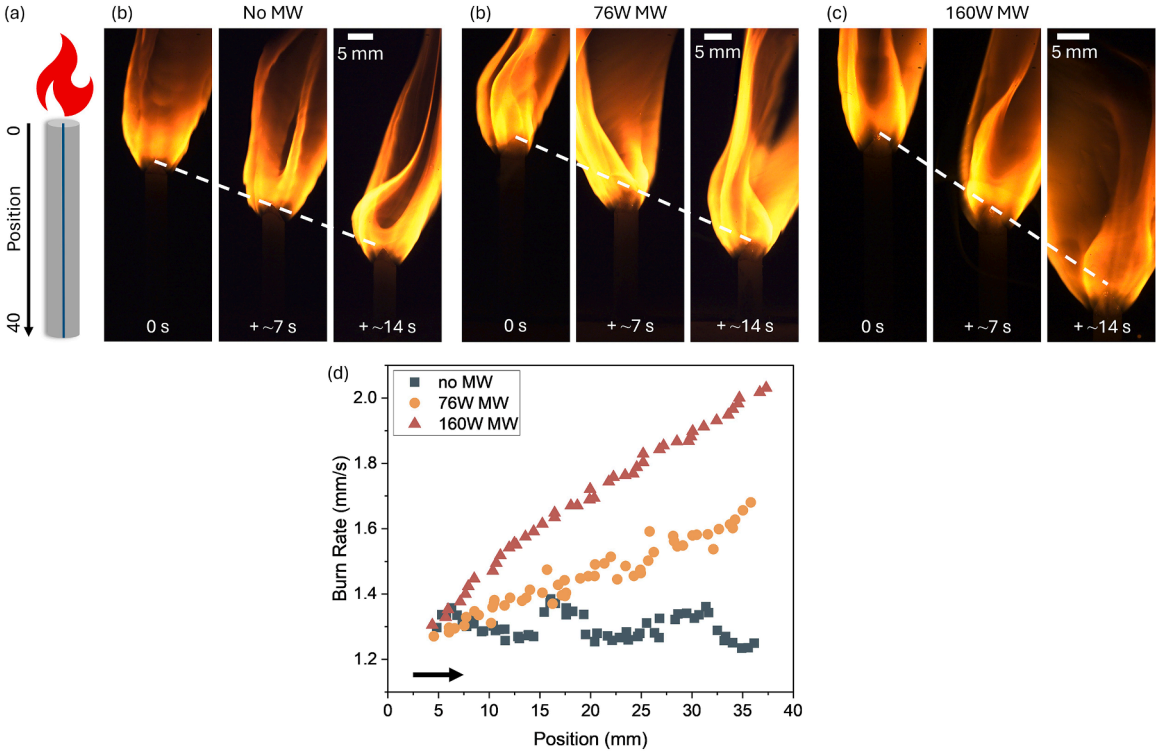

Fig. 2. (a) Scheme of the burning propellant. Images of 40 mm propellants with MW antenna under (b) no MW stimulation, (c) 76 W MW and (d) 160 W MW. (e) Local burn rate of 40 mm propellants with MW antenna and under different MW stimulation power levels. The propagation direction was from left to right as indicated by the arrow.

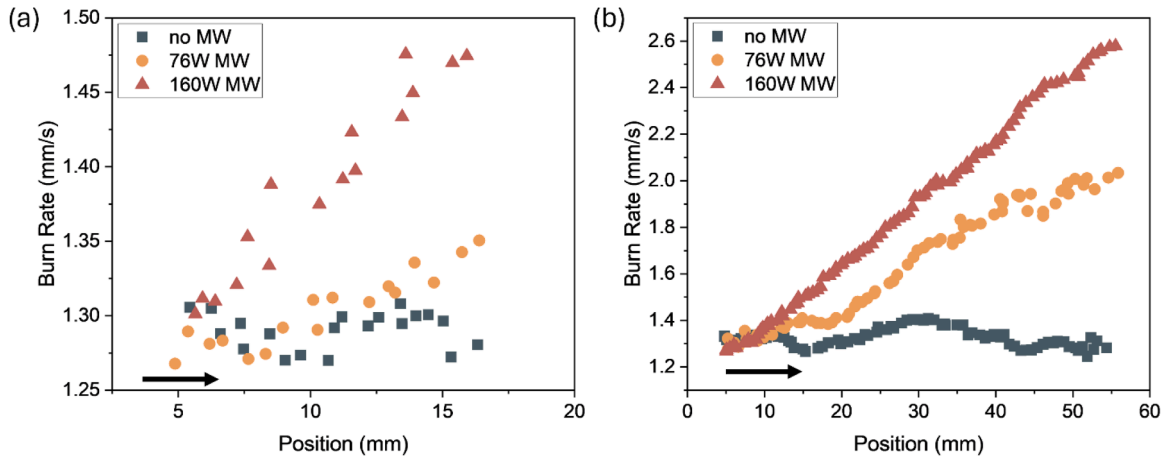

Fig. 3. Local burn rate of (a) 20 mm and (b) 60 mm propellants with MW antenna under different MW power stimulation. The propagation direction was from left to right as indicated by the arrow.

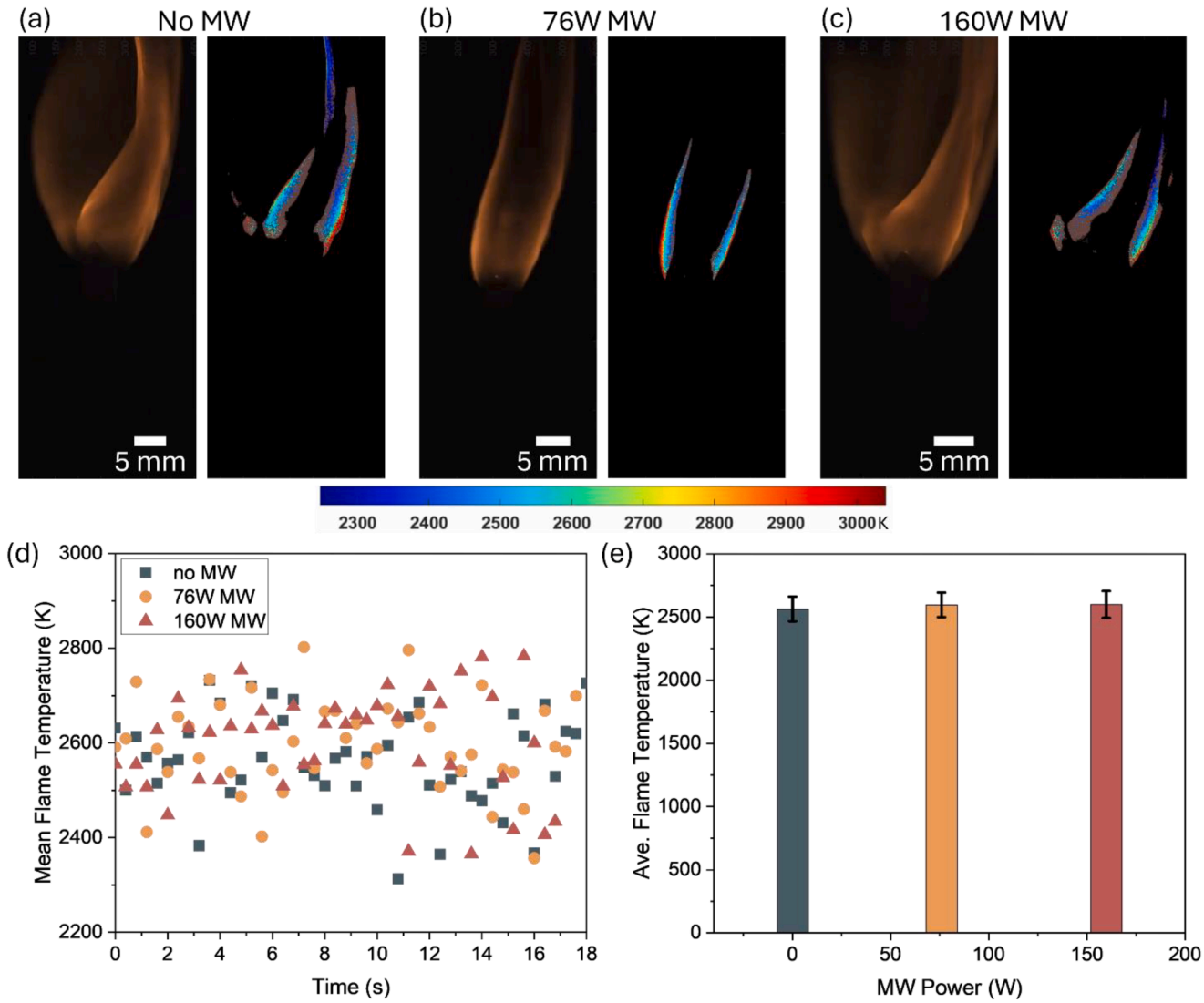

Fig. 4. Pyrometry measurement of flame temperature from 40 mm propellants under (a) no MW stimulation, (b) 76 W MW and (c) 160 W MW. (d) mean flame temperature at each frame and (e) average flame temperature during combustion of 40 mm propellants with MW antenna under MW stimulation at different power levels.

measurements using color camera pyrometry as seen in Fig. 4(a) - (c) [15,16]. The method relies on measuring gray-body emission from particulates generated in the flame. The mean flame temperature as a function of time showed perhaps a slight increase with increasing MW power, but when averaged as seen in Fig. 4(e) these differences are not seen. The average flame temperature is comparable to the calculated adiabatic flame temperature of HTPB (2300 K), but higher than the adiabatic flame temperature of 70 wt. % AP/HTPB propellant (~1300 K) [24,25]. Since these experiments were performed in an ambient environment, AP and surrounding air both act as oxidizers to the HTPB fuel. Similar results were observed for 20 mm and 60 mm propellants (Figure S4). We also note that there were no discernable changes in luminosity of the flame with MW input implying no plasma formation or excitation. This is to be expected, given that the experiment was designed such that the radiating antenna was being consumed at the propellant surface, and thus should have minimal interaction with the gas phase. This point is consistent with minimal change in gas phase temperature observed and that the original premise of the work to restrict MW interaction to the condensed phase.

Since the burn rate is significantly enhanced, but there is no evidence that MW is influencing flame properties, we are left with our original premise that by using a consumable antenna we restrict our energy deposition to the condensed state. But we are still left with explaining the odd behavior that the burn rate accelerates down the length of the wire and that longer strands lead to greater enhancement. One possibility is that the MW is directly heating the wire, but infrared imaging indicates such an effect is minimal. The main source of enhancement left is the heating of the propellant by the emitted MW from the MW antenna. As previously mentioned since AP is MW transparent, the main MW absorption mechanism is the dielectric loss from HTPB, which has hydroxyl groups that rotate and attempt to align with the oscillating electric field, resulting in frictional heating. Fig. 5(a) shows the calculated electrical field in cross-section of a 40 mm propellant with a radiating antenna, and Fig. 5(b) plots the radial distribution of the square of the electric field at different axial positions. We plot E^2 because it is proportional to absorbed power and thus temperature rise [26]. The simulation clearly shows that the highest electric field is located at the tip of the MW antenna and decreases both radially into the propellant and axially down the wire. The radial penetration depth defined as the distance where the electric field falls to ~37 % of its maximum intensity [27]. The penetration depth (δ_p) for materials with low loss tangent ($\tan\delta = \frac{imaginary\ part\ of\ relative\ permittivity\ (\varepsilon_r'')}{real\ part\ of\ relative\ permittivity\ (\varepsilon_r')}$) i.e. weakly absorbing, can be calculated by Eqn. (1) [28]:

$$\delta_p = \frac{\lambda}{2\pi\sqrt{\varepsilon_r'}\tan\delta} \quad (1)$$

Where λ is the wavelength of MW. The calculated penetration depth (~90 cm) is much larger than the propellant diameter suggesting that MW can penetrate the whole radius of the propellant. Fig. 5(c) plots the square of the average electric field along the radius direction as a function of axial location. The results show the highest power absorption of the solid propellant is at the tip of the MW antenna. The absorbed power shows a rapid decline in the top 3 mm region and then gradually decreases along the MW antenna.

We can now calculate the absorbed power (Q) within the solid propellant:

$$Q = \left[\int_0^x (ave\ E)^2 dx\right] \cdot t \quad (2)$$

Where $(ave\ E)^2$ is the square of the average electric field intensity along the radius direction as plotted in Fig. 5(c), x is the axial position of the burning surface, and t is the burn time to position x. The absorbed power during the combustion process was normalized by the maximum absorbed power by 160 W MW stimulation and plotted in Fig. 6. We can see that the absorbed power increases linearly with propellant burn time (MW stimulation time). This also corresponds closely to the observation that the burn rate increases with axial location. From this we may conclude: the solid propellant is heated by the emitted electric field from the embedded MW antenna, and not by heating of the wire, or any MW coupling to the gas-phase flame. The electric field is focused on the tip region of the MW antenna, which is consumed with the burning surface so that the peak field is maintained at the burning surface. The absorbed power of the solid propellant by MW stimulation linearly increases with burn time and corresponds to the linear increase in local burn rate.

3.3. MW heating in the condensed phase

The combustion of solid propellants is sensitive to the microstructure of the condensed phase since cracks or voids can cause the burning surface to propagate in an undesired direction and severely interfere with the stability of the solid propellant [29–31]. Since low temperature decomposition of AP occurs at ~300 °C and the decomposition of HTPB at ~280 °C, gas species can generate pores inside the solid propellants [32,33]. Thus it is important that any MW heating should not exceed or even approach these critical temperatures. To evaluate the heating effect by the MW antenna, the 60 mm samples were quenched after 55 mm of

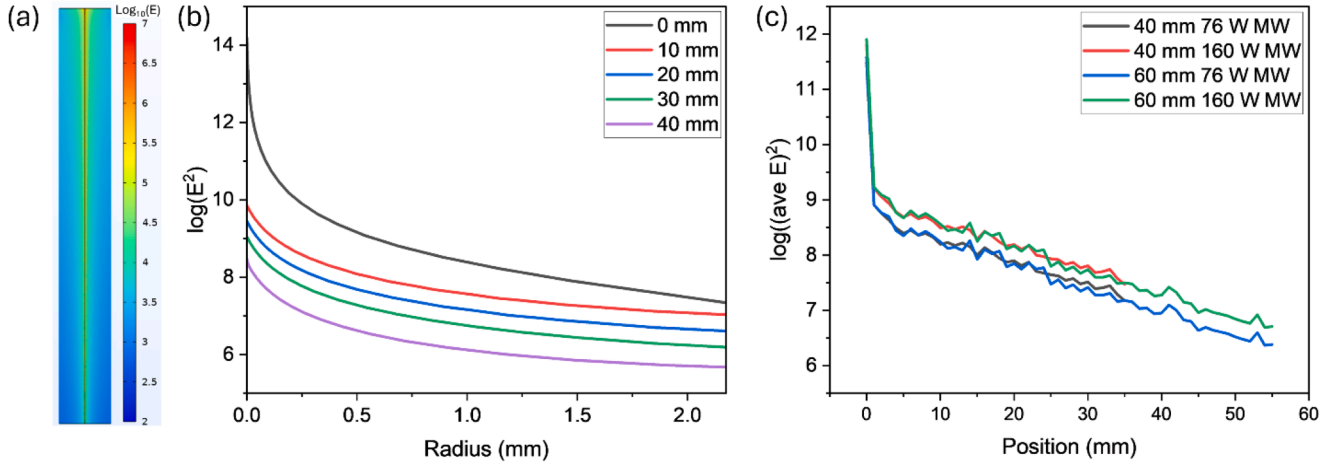

Fig. 5. (a) Electric field (unit: V/m) distribution in the cross-section of 40 mm propellant with embedded MW antenna. (b) The square of electric field intensity along the radius at different axial position. (0 mm represents the top surface) (c) The square of the average electric field intensity along the radius direction at different propellant axial positions.

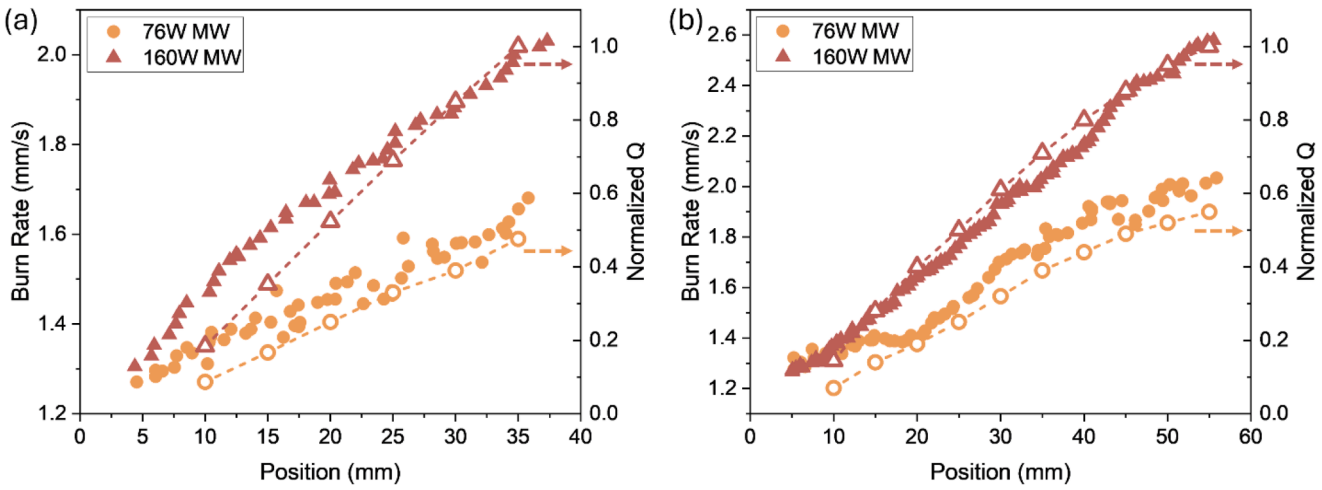

Fig. 6. Normalized absorbed power by the solid propellant from the emitted electric field of (a) 40 mm and (b) 60 mm propellant.

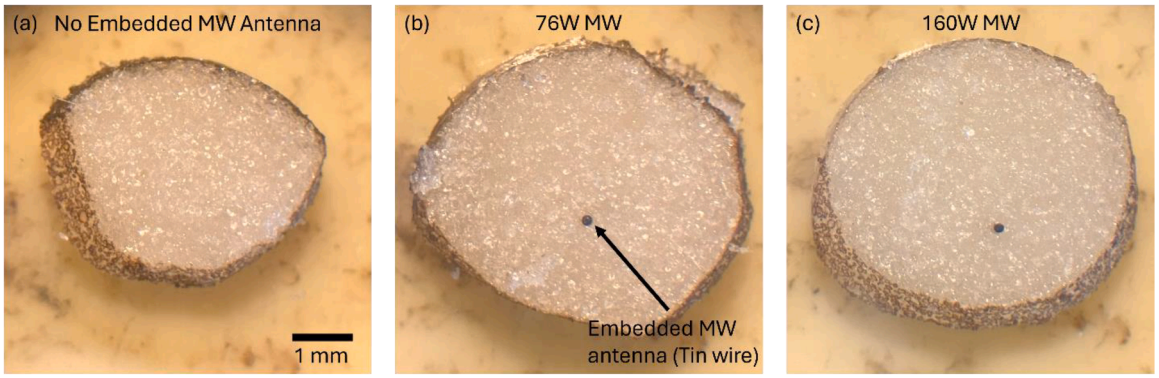

Fig. 7. Quenched 60 mm propellant with (a) no embedded MW antenna, (b) embedded MW antenna at 76 W and (c) embedded MW antenna at 160 W.

burn (~5 mm remaining) at different power levels. Fig. 7 shows the cross-section slice of the quenched propellant with and without MW stimulation. We observe no obvious changes such as cracks or voids, and the antenna appears to be conformally attached to the propellant. This indicates that the heat transfer by the tin wire used in this experiment was limited by its thin diameter and low thermal conductivity and confirms that the wire itself has no influence on the burn rate.

4. Conclusions

The premise of this work was to focus microwave energy directly to the reaction front via a consumable wire antenna. Due to the low thermal conductivity of Tin and thin diameter of the wire, the embedding wire itself did not affect the propellant burn rate. Video analysis coupled with color camera pyrometry indicated that MW power could increase burn rate in our samples up to a factor of 2, but did not show any indication of changes to flame temperature or flame structure. This latter point showed that the solo interaction of MW's was with the condensed phase HTPB which is a weak MW absorber. Electric field simulation of the MW antenna within the propellant indicated that the burn rate increase is related to the heating of the HTPB. The absorbed MW power in solid propellant as conjectured is focused on the burning surface during combustion and decreases along the MW antenna. Quenching studies of the propellant suggested that the MW power used in this experiment was not sufficient to cause any noticeable changes to the composite prior to combustion. This study demonstrated a novel and safe method to modulate the burn rate of solid AP/HTPB propellant by focusing MW energy at the burning surface of propellant.

Novelty and significance statement

We propose a novel method to modulate the burn rate of AP/HTPB propellants by MW energy. An MW antenna was embedded into the propellants and the burn rate increased significantly. Simulation and pyrometry measurement suggested that the MW energy was delivered directly to the burning surface of propellant. This study offers the potential to throttle solid propellants by focusing MW energy on the burning surface.

CRediT authorship contribution statement

Keren Shi: Writing – original draft, Formal analysis, Data curation. **Erik Hagen:** Writing – review & editing, Data curation. **Yujie Wang:** Data curation. **Michael R. Zachariah:** Writing – review & editing, Supervision, Project administration, Methodology, Investigation, Funding acquisition, Conceptualization.

Declaration of competing interest

On behalf of all the authors, we declare no conflict of interest. This work is original and has not been considered for publication elsewhere.

Acknowledgements

The authors thank the support from the Air Force Office of Scientific Research (AFOSR).

Supplementary materials

Supplementary material associated with this article can be found, in the online version, at doi:10.1016/j.combustflame.2025.114304.

References

[1] A. Davenas, Development of modern Solid propellants, J PROPUL POWER 19 (2003) 1108–1128.
[2] V.A. Babuk, A. Glebov, V.A. Arkhipov, A.B. Vorozhtsov, G.F. Klyakin, F. Severini, L. Galfetti, L.T. DeLuca, Dual-oxidizer solid rocket propellants for low-cost access to space, Tenth Int. Workshop Combust. Propuls. (2005) 15, paper.
[3] X. Wang, C. Pei, F. Xu, X. Wu, H. Li, N. Yang, D. Liu, S. Xu, Experimental and simulative thermal stability study of HTPE solid propellants in different scales, Case Stud. Therm. Eng. 28 (2021) 101566.
[4] V.A. Babuk, V.A. Vassiliev, V.V. Sviridov, Propellant formulation factors and metal agglomeration in combustion of aluminized solid rocket Propellant, COMBUST SCI TECHNOL 163 (2001) 261–289.
[5] M.W. Beckstead, A model for solid propellant combustion, Symp. (Int.) Combust 18 (1981) 175–185.
[6] A. Kakami, S. Terashita, T. Tachibana, Application of laser-assisted combustion to solid propellant for space propulsion, in: 46th AIAA/ASME/SAE/ASEE Joint Propulsion Conference & Exhibit, 2010, pp. 2010–6584, paper.
[7] S. Ikuta, D. Haraguchi, Y. Yano, A. Kakami, Performance of a throttleable solid propellant microthruster using laser heating, Aerosp. Tech. Jpn. 19 (2021) 598–603.
[8] K.E. Uhlenhake, M. Gomez, D.N. Collard, M. Örnek, S.F. Son, Laser ignition of solid propellants using energetic nAl-PVDF optical sensitizers, COMBUST FLAME 254 (2023) 112848.
[9] S.J. Barkley, K. Zhu, J.E. Lynch, J.B. Michael, T.R. Sippel, Microwave plasma enhancement of multiphase flames: on-demand control of solid propellant burning rate, COMBUST FLAME 199 (2019) 14–23.
[10] J.A. Lajoie, B. Jones, A.R. Lawrence, S.J. Barkley, T.R. Sippel, On-demand microwave growth of porosity within a granular composite energetic material: void formation via a dielectric loss phase change binder additive for propellant burning rate control, PROPELL EXPLOS PYROT 49 (2024) e202300229.
[11] K. Shi, Y. Wang, F. Xu, M.R. Zachariah, Remote microwave heating and ignition with an embedded receiving antenna within nanocomposites, CHEM ENG SCI 280 (2023) 118948.
[12] K. Shi, Y. Wang, M.R. Zachariah, Microwave antenna focusing for spatially resolved modulation of burn rate, CHEM ENG J 492 (2024) 152192.
[13] J.Yang Wang, W. Cheng, J. Zou, D. Zhao, Progress on polymer composites with low dielectric constant and low dielectric loss for high-frequency signal transmission, Front. Mater 8 (2021) 774843.
[14] K. Hasue, M. Tanabe, N. Watanabe, S. Nakahara, F. Okada, A. Iwama, Initiation of some energetic materials by microwave heating, PROPELL EXPLOS PYROT 15 (1990) 181–186.
[15] R.J. Jacob, D.J. Kline, M.R. Zachariah, High speed 2-dimensional temperature measurements of nanothermite composites: probing thermal vs. Gas generation effects, J APPL PHYS 123 (2018) 115902.
[16] H. Wang, B. Julien, D.J. Kline, Z. Alibay, M.C. Rehwoldt, C. Rossi, M.R. Zachariah, Probing the reaction front of nanolaminates at ∼μs time and ∼μm spatial resolution, J. Phys. Chem. C 124 (25) (2020) 13679–13687.
[17] COMSOL Multiphysics® v. 5.6. www.comsol.com. COMSOL AB, Stockholm, Sweden.
[18] C. Dennis, B. Bojko, On the combustion of heterogeneous AP/HTPB composite propellants: a review, Fuel 254 (2019) 115646.
[19] A.L. HigginbothamDuque, W.L. Perry, C.M. Anderson-Cook, Complex microwave permittivity of secondary high explosives, PROPELL EXPLOS PYROT 39 (2014) 275–283.
[20] S. Isert, C.D. Lane, I.E. Gunduz, S.F. Son, Tailoring burning rates using reactive wires in composite solid rocket propellants, P COMBUST INST 36 (2017) 2283–2290.
[21] L.H. Caveny, R.L. Glick, Influence of embedded metal fibers on solid- propellant burning rate, J SPACECR. ROCKETS 4 (1967) 79–85.
[22] C. Shuling, L. Fengsheng, Influence of long metal wires on combustion of double-base propellants, COMBUST FLAME 45 (1982) 213–218.
[23] S. Hammack, X. Rao, T. Lee, C. Carter, Direct-coupled plasma-assisted combustion using a microwave waveguide torch, IEEE T PLASMA SCI IEEE 39 (2011) 3300–3306.
[24] G. Young, S. Hromisin, S. Loeffler, T.L. Connell, Effect of oxidizer type on solid fuel combustion, J PROPUL POWER 36 (2020) 248–255.
[25] N. Kubota, Survey of rocket propellants and their combustion characteristics, in: K. Kuo (Ed.), Fundamentals of Solid-Propellant Combustion, American Institute of Aeronautics and Astronautics, 1984.
[26] C. Gabriel, S. Gabriel, E.H. Grant, E.H. Grant, B.S.J. Halstead, D. Michael P. Mingos, Dielectric parameters relevant to microwave dielectric heating, CHEM SOC REV 27 (1998) 213.
[27] S. Horikoshi, R.F. Schiffmann, J. Fukushima, N. Serpone, Microwave Chemical and Materials Processing, Springer Singapore, Singapore, 2018.
[28] F.T. Ulaby, U. Ravaioli, Fundamentals of Applied Electromagnetics, 7th edition, Pearson, Boston, U.S., 2015.
[29] C.T. Liu, Crack growth behavior in a solid propellant, ENG FRACT MECH. Vol. 56 (1) (1997) 127–135.
[30] F. Xu, N. Aravas, P. Sofronis, Constitutive modeling of solid propellant materials with evolving microstructural damage, J MECH PHYS SOLIDS 56 (2008) 2050–2073.
[31] J. Wang, H. Qiang, Z. Wang, S. Li, Numerical study of mechanical properties of composite solid propellant with initial defects, J PHYS CONF SER J 1634 (2020) 012146.
[32] P.N. Dave, R. Sirach, R. Thakkar, Thermal decomposition and kinetic investigation of AP and AP based composite solid propellant in the presence of nickel ferrite additive, J. Mater. Res. Technol. 19 (2022) 4183–4196.
[33] Y.K. Sinha, B.T.N. Sridhar, M. Santhosh, Thermal decomposition study of HTPB solid fuel in the presence of activated charcoal and paraffin, J Therm Anal Calorim 119 (2015) 557–565.